Supplementary figures

"Ten-Eleven Translocation promotes muscle progenitor maintenance through cell-autonomous and niche-dependent mechanisms"

Gerdy et al.

A

Library	Total Reads	Aligned Reads	Putative Cells	Reads per Cell	Molecules per Cell
WT1	278,267,794	226,707,309	4,245	49,570	22,127
WT2	269,804,526	222,473,268	4,361	47,803	23,079
TET1	259,561,689	212,965,575	3,776	50,655	24,568
TET2	251,854,353	205,646,533	3,625	51,548	24,067

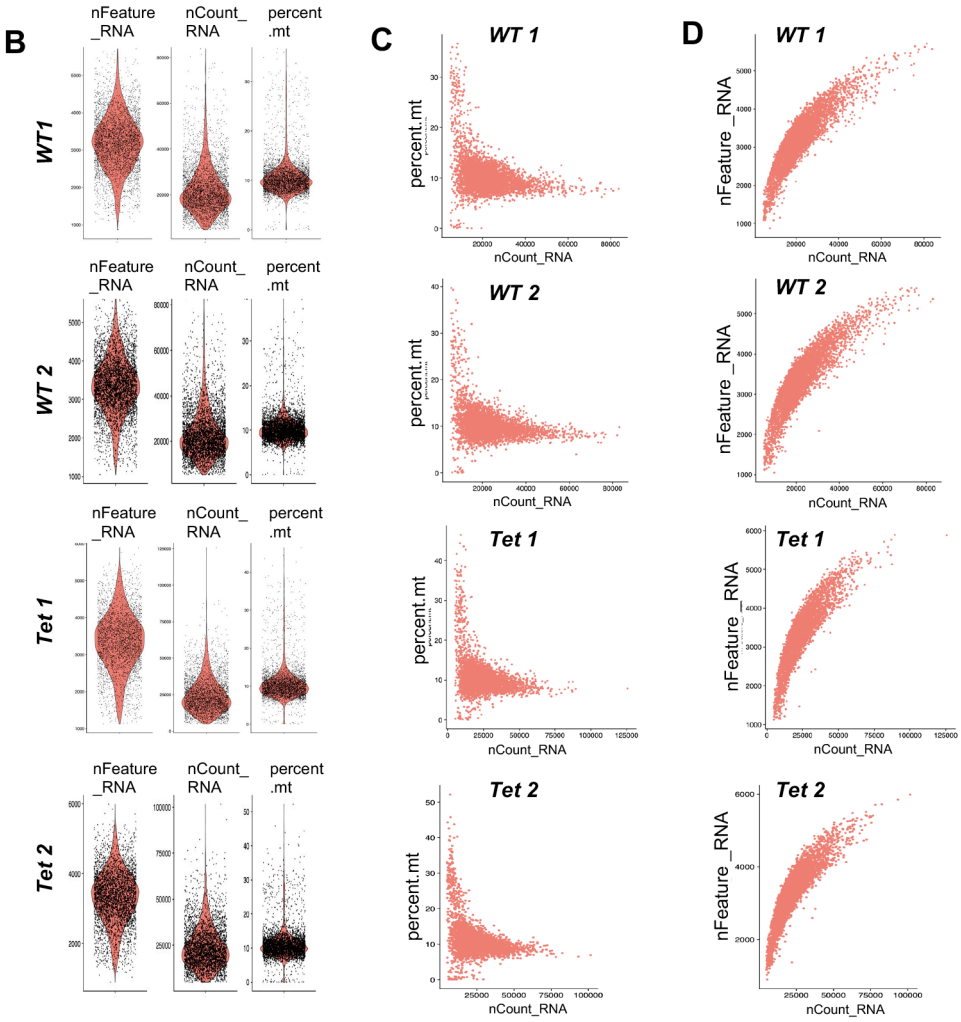

Figure S1. (A) Key features of the single-cell RNA sequencing output. **(B)** Repartition of the total number of genes expressed per cell (nFeature_RNA), the total number of RNA molecules per cell (nCount_RNA) and the percentage of

mitochondrial RNA (percent.mt) for each of wild-type *(WT1, WT2*) and *Tet*^{null} (*Tet1*, *Tet2*) biological replicates. (**C, D)** Pre-processing steps for the selection of the single cells. Cells with more than 15% of mitochondrial reads (C) and cells with more than 5.000 or less than 1.000 expressed genes (D) were discarded. **(E, F)** Correlation of gene expression between independent replicates of wild-type (E) or *Tet*^{null} (F) scRNA-seq data. The Pearson's correlation coefficients are indicated.

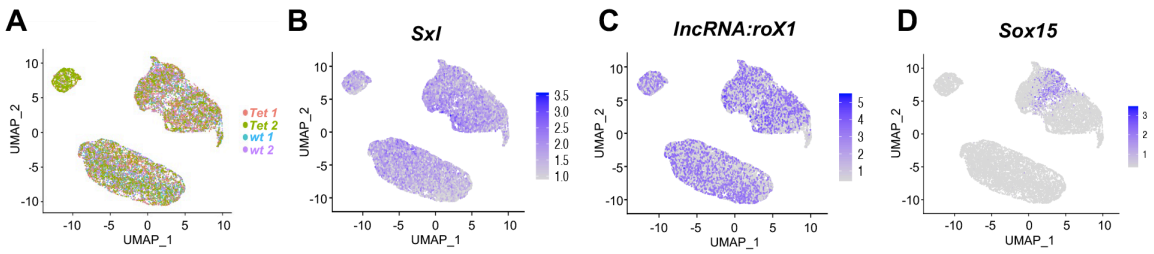

Figure S2. (A) UMAP of the harmonized single cells data. Each colour corresponds to a different sample. Wild-type replicate 1: blue, replicate 2: purple. *Tet*^{null} replicate 1: red, replicate 2: green. **(B-D)** UMAPs of the harmonized single-cell data showing the expression of the female gene *Sex lethal* (*Sxl*) (B), the male specific gene *lncRNA:roX1* (C) and the hinge marker *Sox15* (D).

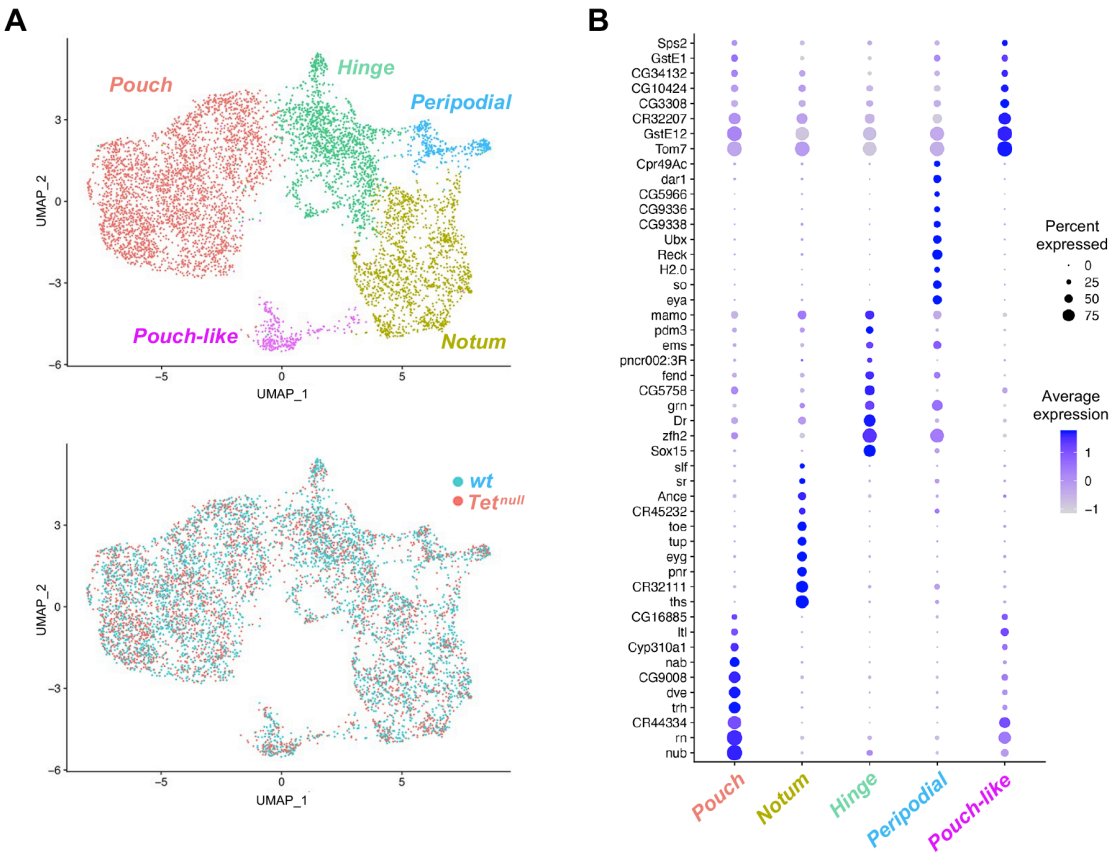

Figure S3. **(A)** UMAPs of the epithelial cells using higher resolution for the unsupervised clustering of the harmonized single-cell datasets. Top panel: clusters are coloured by identities and annotated based on the expression of marker genes. Lower panel: cells are coloured by genotype. Wild-type: blue. *Tet*^{null}: red. **(B)** Dot plot showing the expression levels of the top markers identified for the pouch, hinge, notum, peripodial and “pouch-like” cells.

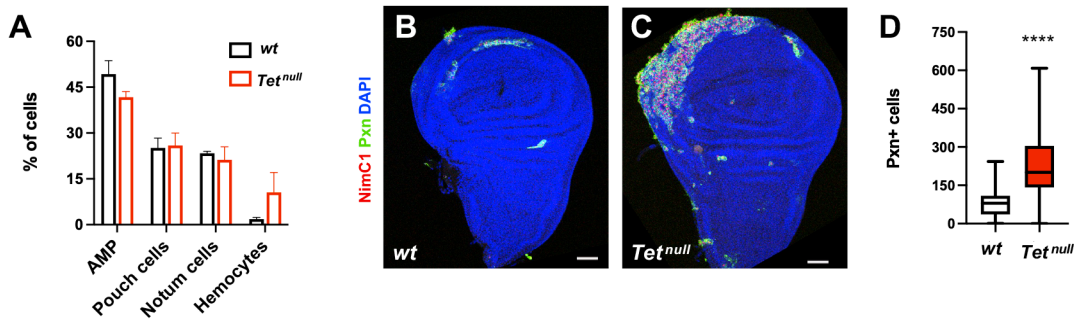

Figure S4. (A) Proportion of each cell type identified by scRNA-seq in wild-type or *Tet*^{null} wing discs. Mean and standard deviations are shown. **(B, C)** Confocal images of wing discs from wild-type (B) or *Tet*^{null} (C) third instar larvae showing the expression of the blood cell markers NimC1 (green) and pxn-RedStinger (red). Nuclei were stained with DAPI. Scale bar: 50 µm. **(D)** Quantification of the number of hemocytes (Pxn^{+} cells) associated wild-type or *Tet*^{null} wing disc. ****: $P < 0.0001$ (Student's t-test).

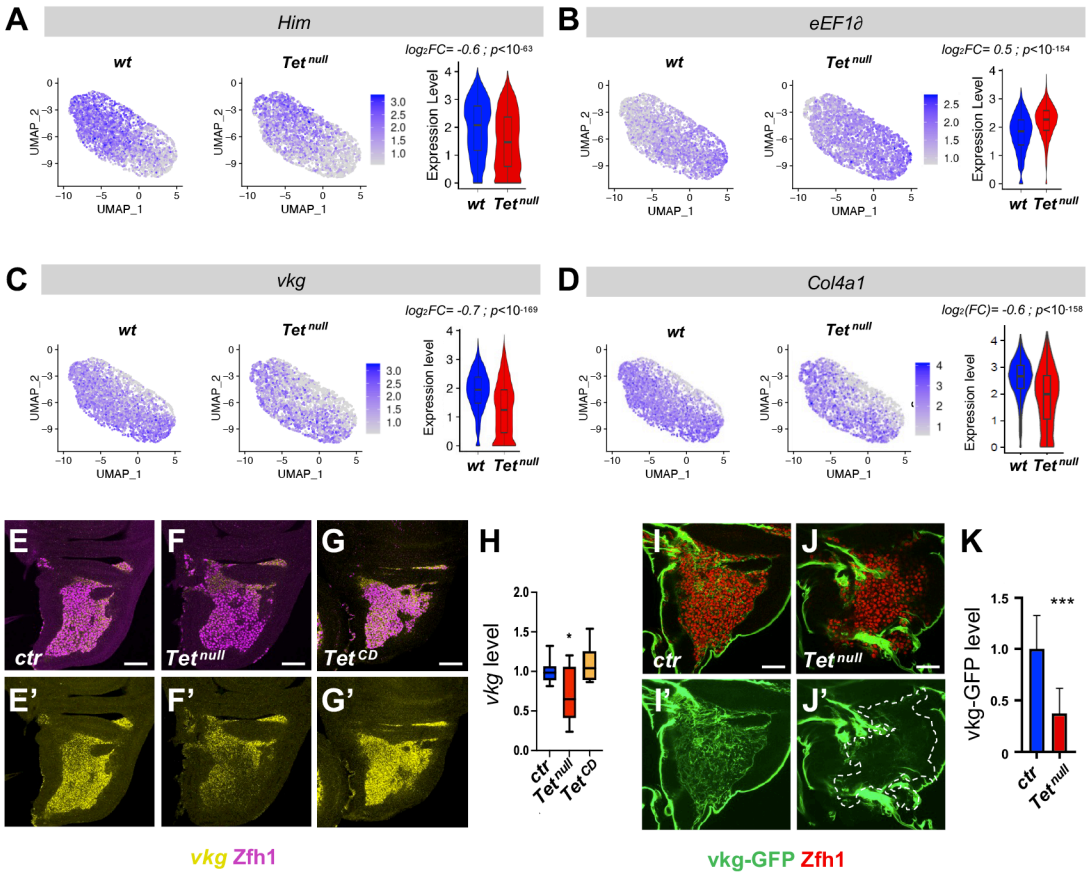

Figure S5. (A-D) UMAPs and violin plots showing the expression of *Him* (A), *eEf1∂* (B), *vkg* (C) and *Col4a1* (D) in wild-type or *Tet*^{null} AMPs. **(E-G)** Expression of Zfh1 (purple) and *vkg* (yellow) was assessed by immunostaining and FISH, respectively, in wing disc of wild-type (E), *Tet*^{null} (F) or *Tet*^{CD} (G) larvae. (E'-G'): yellow channel (*vkg*). Scale bar: 50 µm. **(H)** Expression level of *vkg* in Zfh1^{+} cells (relative to wild-type) in the different genotypes. Mean fluorescent intensity per µm^3 and sd are represented. *: $P < 0.05$ (Mann-Whitney t-test). **(I, J)** Expression of Zfh1 (red), and vkg-GFP (green) in wing disc of wild-type (I) or *Tet*^{null} (J) larvae. Scale bar: 50 µm. (I', J'): green channel only (vkg-GFP). **(K)** Corresponding quantification of vkg-GFP fluorescence level in Zfh1^{+} cells (relative to wild-type). Mean fluorescent intensity per µm^3 and sd are represented. ***: $P < 0.001$ (Student's t-test).

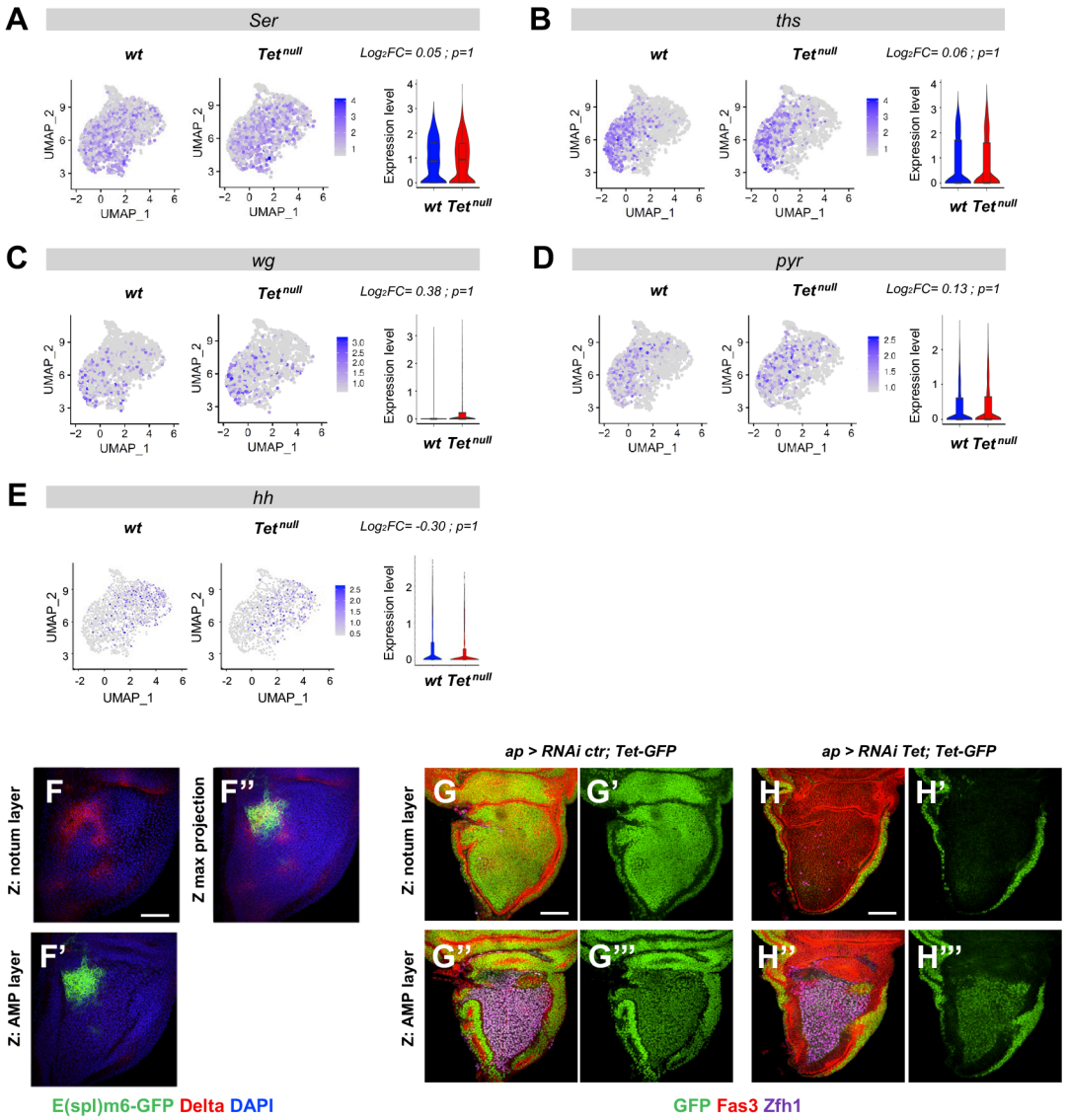

Figure S6. **(A-E)** UMAPs and violin plots showing the expression of *Ser* (A), *ths* (B), *wg* (C), *pyr* (D) and *hh* (E) in notum cells of wild-type or *Tet*^{null} larvae. **(F)** Immunostaining against Delta (red) and GFP in the wing disc of *E(spl)m6-BFM-GFP* larvae. Nuclei were stained with DAPI. Scale bar: 50 µm. (F) confocal view of the epithelial layer. (F') confocal view of the AMP layer. (F'') Z-max projection. **(G-H)** Immunostaining against Fas3 (epithelium; red), Zfh1 (AMP; purple) and GFP (green) in wing disc of *Tet-GFP* larvae expressing the indicated RNAi under the control of *ap-GAL4*. Scale bar: 50 µm. (G, G', H, H') confocal view of the epithelial

layer. (G”, G”’, H”, H’”) confocal view of the AMP layer. (G’, G’”, H’, H’”) only the green channel (TET-GFP) is shown.

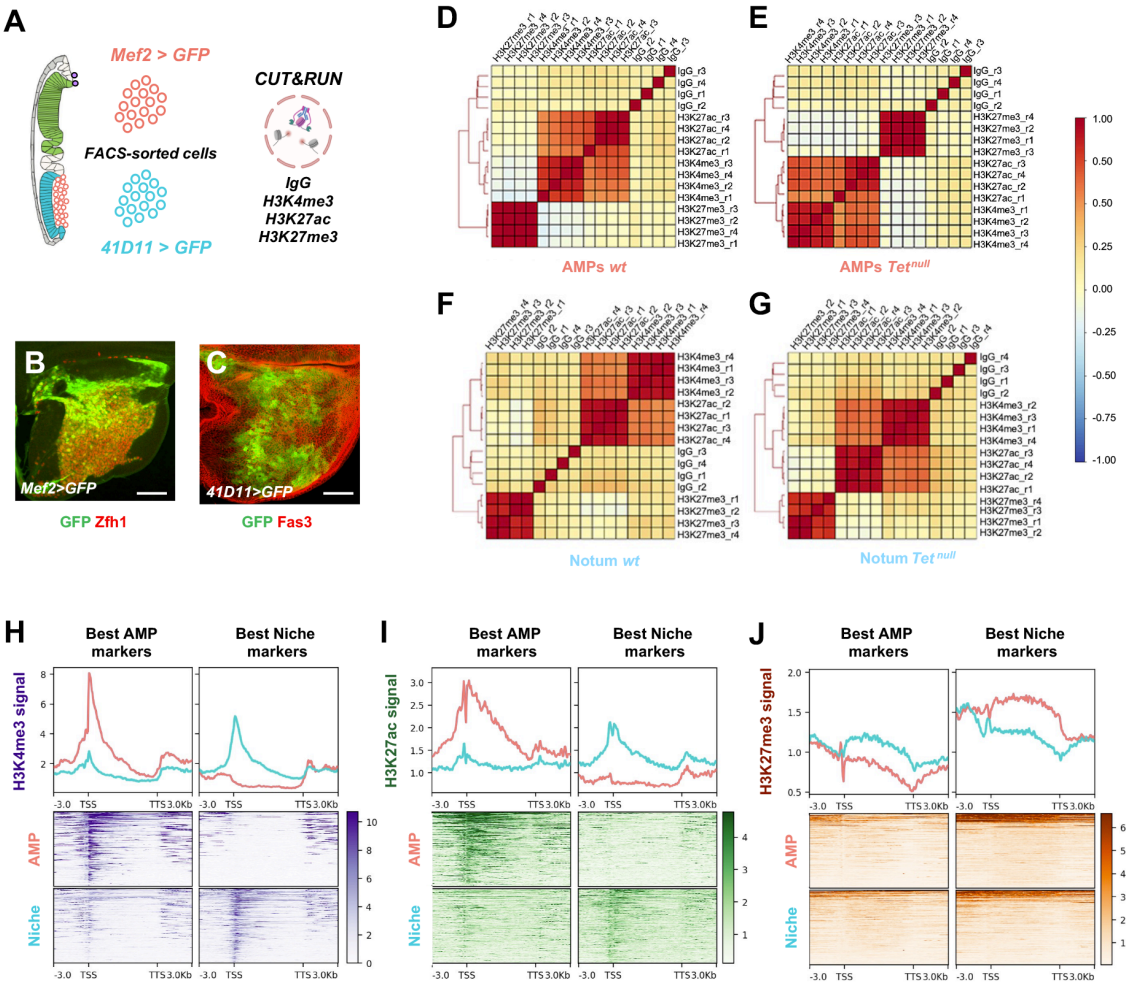

Figure S7. (A) Schematic representations of wing disc-associated cells and CUT&RUN experimental design. GFP-positive AMPs or notum cells were purified by FACS from wild-type or *Tet*^{null} third instar larval wing discs using the *Mef2-Gal4* or *41D11-Gal4* driver, respectively. **(B, C)** Immunostainings against GFP (green) and Zfh1 (B, red) or Fas3 (C, red) in wing discs of *Mef2-GAL, UAS-GFP (A) or 41D11-GAL4, UAS-GFP* larvae. Scale bar: 50 µm. (B) confocal view of the AMP layer. (C) confocal view of the epithelial layer. **(D-G)** Hierarchically clustered correlation matrixes of CUT&RUN profiling in biological quadruplicates for H3K4me3, H3K27ac and H3K27me3 modification marks and a negative control (IgG) in AMPs (D, E) or notum cells (F, G) isolated by FACS from wild-type (D, F) or *Tet*^{null} (E, G) larvae. **(H-J)** H3K4me3 (H), H3K27ac (I) and H3K27me3 (J) histone

71 modification profiles for the top 200 differentially expressed genes between AMPs
72 or niche cells in each of these two cell populations. TSS: transcription start site. TTS:
73 transcription termination site.

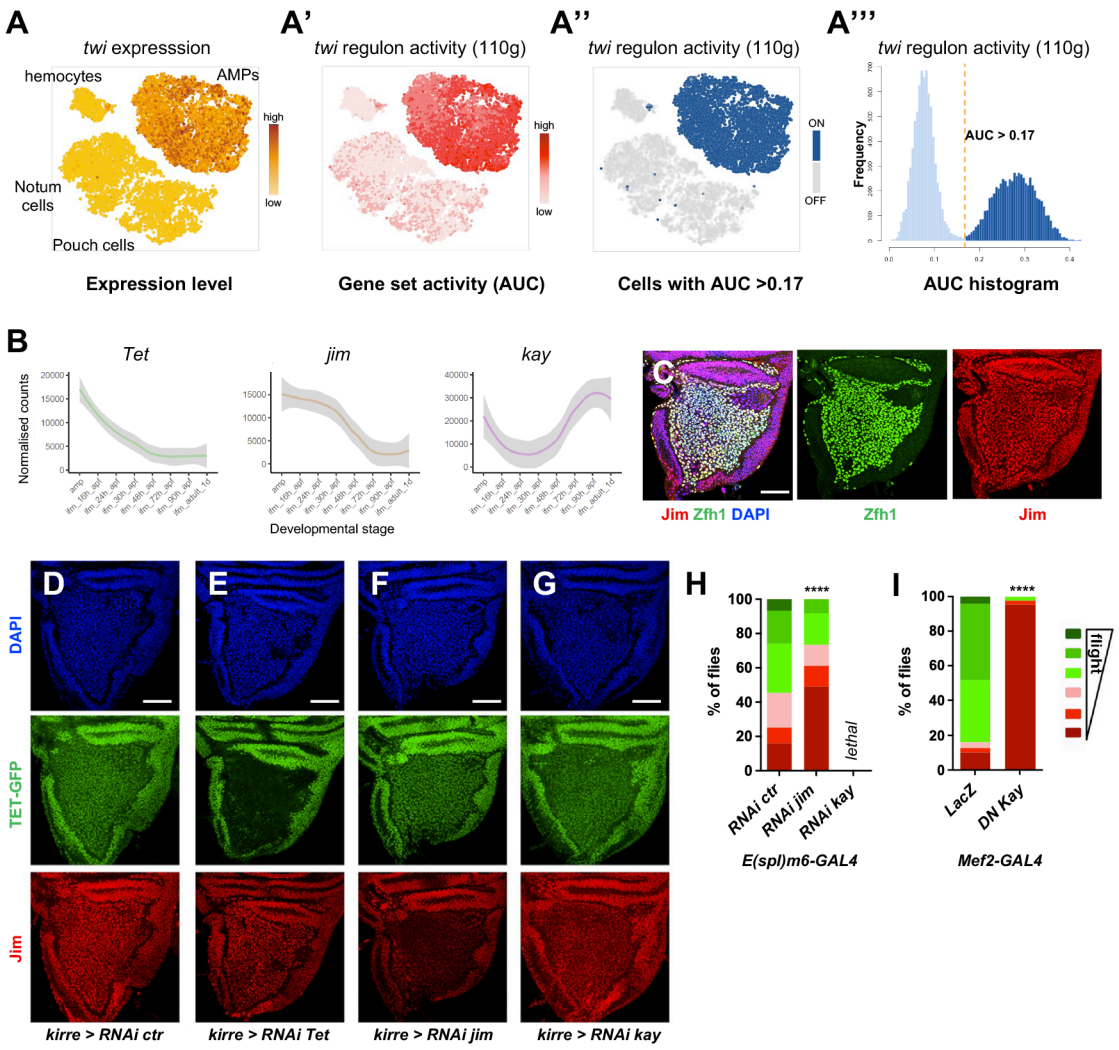

Figure S8. (A) SCENIC-based analysis of Twi activity in the integrated scRNA-seq dataset. (A-A'') Projection of *twi* expression (A), Twi regulon level (A') and Twi regulon activity (A'') on the wing disc UMAP. (A''') Histogram showing Twi regulon level (AUC score) in wing disc cells. All cells with an AUC > 0.17 were classified as positive for Twi regulon activity in A''. **(B)** Expression dynamic of *Tet* (left panel), *jim* (central panel) and *kay* (right panel) during IFM development. Time-course RNA-seq data on developing IFM (GSE107247) were used to analyse mRNA levels from the third instar larval stage to adulthood using DESeq2. **(C)** Immunostaining against Jim (red) and Zfh1 (green) in wild-type third instar wing disc larvae. **(D-G)** Immunostaining against Jim (red) and GFP (green) in the wing disc of *Tet-GFP* third

instar larvae expressing the indicated RNAi under the control of *kirre-GAL4*. (C-G) Confocal views of the AMP cell layer. Nuclei were stained with DAPI. Scale bar: 50 µm. **(H, I)** Flight performance assays on 1-week-old males expressing the indicated transgenes under the control of *E(spl)m6-BFM-GAL4* (raised at 30°C) (H) or *Mef2-GAL4* (I). DN Kay: dominant-negative form of Kay. The percentage of flies landing in each of the 6 zones is indicated. ****: $P < 0.0001$ (Fisher's exact test).

Supplementary table 1. List of markers in scRNA-seq clustering. Sheet 1: wing disc clustering. Sheet 2: epithelial cell subclustering. Sheet 3: AMP subclustering.

Supplementary Table 2. List of differentially expressed genes between wild-type and Tet^{null} in AMPs, pouch cells, notum cells, hemocytes, AMP subsample and epithelial cells.

Supplementary Table 3. Gene Ontology enrichment analyses between wild-type and Tet^{null} AMPs.

Supplementary Table 4. Differential expression analyses on cell-cycle-associated genes between wild-type and Tet^{null} AMPs or epithelial cells.

Supplementary Table 5. Gene Ontology enrichment analyses between wild-type and Tet^{null} notum cells.